

RESPONSE OF SiC/SiC TO TRANSIENT THERMAL CONDITIONS: A REVIEW - R. H. Jones (Pacific Northwest National Laboratory)*

OBJECTIVE

The objective of this review is to evaluate the database on thermal shock and thermal fatigue effects in SiC/SiC composites, to determine if there is sufficient data to predict the impact of thermal transients on their properties and if so to predict this behavior.

SUMMARY

The database on thermal shock behavior of SiC/SiC composites is very limited. The existing data suggests continuous fiber ceramic matrix composites, such as SiC/SiC, exhibit very good thermal shock characteristics but most data was obtained for $-\Delta T$ conditions as a result of quenching from an elevated temperature. Thermal shock in a fusion energy system will result from plasma discharge and will result in a $+\Delta T$. One study was reported for SiC/SiC composites given a $+\Delta T$ with no loss in strength following 25 cycles at a heating rate of 1700°C/s . Monolithic SiC failed in 1.5 cycles at a heating rate of 1400°C/s . Thermal fatigue test results also suggest that SiC/SiC composites will exhibit little or no degradation for 100's of cycles. It was estimated that radiation could, in an extreme case, cause a reduction in the thermal shock performance from a calculated ΔT_c of 957K to about 300K if the fiber strength is reduced by 50%. Newer composites with greater radiation resistance should have a much smaller change in the ΔT_c .

PROGRESS AND STATUS

Background

Transient thermal conditions will occur in a fusion energy system from both the system duty cycle and plasma discharge processes. Shutdown of the system for either scheduled or unscheduled maintenance will result in a temperature decrease of the blanket that inevitably will cause some stress build-up in the material. The stress magnitude will be dependent on the cooling rate and thermal gradients. This type of cycle is usually referred to as thermal-fatigue, involves the entire blanket and is measured in the laboratory in simulated thermal cycling tests or low-cycle fatigue (mechanical) tests. Start-up will also induce stress of the opposite sign to that produced by shutdown and may relax the cool-down stresses. Plasma discharge will induce a rapid heating of a small volume of plasma-facing material and some larger volume of blanket material. Transmission of the thermal energy through the blanket and therefore the temperature change and stress response will be very design and material dependent.

Cooling the surface of a material faster than the interior results in a surface tensile stress while heating the surface of a material faster than the interior results in a surface compressive stress. The heating or cooling rate and ΔT determine the magnitude of the stress. The maximum temperature can also affect the material microstructure and properties. The magnitude of the stress is determined by the heating rate through the resulting thermal gradient. For thermal shock conditions, the thermal diffusivity may be sufficiently slow that a thermal gradient is not established in the short-term such that the surface stress is determined by the energy deposition and resulting surface temperature and not by a thermal gradient. Assuming that the residual stresses have relaxed to zero at the operating temperature, cooling during a shutdown will result in a surface tensile stress and a plasma discharge in a surface compressive stress. In composite materials, internal stresses are also determined by the differential thermal expansion between the

*Pacific Northwest National Laboratory (PNNL) is operated for the U.S. Department of Energy by Battelle Memorial Institute under contract DE-AC06-76RLO-1830.

fiber and matrix so that the analysis of thermal stress is more complex than for a monolithic material. It is conceivable that the internal stresses could reverse the thermal gradient stress.

Thermal Shock Behavior of Ceramic Composites

Thermal shock behavior is an important aspect of monolithic ceramic materials because their low fracture toughness, low thermal conductivity and high elastic modulus renders them susceptible to failure under transient thermal conditions. Thermal shock studies of monolithic ceramics cover a range of testing methods, failure analysis methods and models that have been reviewed by Wang and Singh [1].

Models of thermal shock fall into two categories: 1) those based on fracture resistance (initiation of cracks on the surface) and 2) crack propagation resistance. Fracture resistance models predict a thermal shock resistance parameter R that is equal to the ΔT_c the maximum allowable temperature difference to which a body can be subjected without the initiation of fracture under both steady state heat flow or severe transient thermal conditions. This parameter is defined by Equation 1:

$$\Delta T_c = R = \sigma_t (1-\nu)/\alpha E \quad (1)$$

where σ_t is the material's tensile strength, E is the Young's modulus, α is the coefficient of thermal expansion and ν the Poisson's ratio. The fracture strength can be considered equal to the tensile strength in brittle materials. For this analysis, the fracture strength is equal to the thermal stress on the surface at ΔT_c . There are several variants of this parameter for different heating conditions. The maximum allowable black body radiation to which opaque materials can be subjected is given by R_{rad} , the maximum allowable black body temperature to which semitransparent materials can be subjected by R_{trans} , and the case where a material is undergoing creep by R_{cr} .

The crack propagation resistance models rely on the available amount of elastic energy stored in the material that is available for crack propagation. This is similar to the Griffith fracture criterion that balances the elastic energy available for crack propagation with the surface energy required to advance the crack. An equation for R''' that defines the minimum elastic energy at fracture available for crack propagation as:

$$R''' = E/\sigma_t^2 (1-\nu) \quad (2)$$

where the parameters have the same meaning as in Equation 1. It is important to note that these two failure criteria give different responses to fracture strength and elastic modulus. Material with a high fracture strength and low Young's modulus is desired to optimize R , but a material with a low fracture strength and high Young's modulus is needed to optimize R''' .

Quenching into liquid media is the most common method for introducing a negative ΔT with common quenching media being water, silicone oil, liquid metal, methyl alcohol and glycerine. Methods for producing a positive ΔT include heating a sample with a plasma jet, laser, tungsten halogen lamp, electron beam, hot gas jet, arc discharge and hydrogen-oxygen flame from a rocket engine. A number of methods are used to assess the thermal shock damage including: 1) measuring the dynamic moduli of elasticity using ultrasonic waves, 2) measuring the Young's modulus by the mechanical resonance method, 3) measuring the change in specific damping capacity, 4) monitoring the change in the spectra of ultrasonic pulses passed through a specimen, 5) recording acoustic emission signals during quenching and 6) measuring the thermal diffusivity change. Each technique has advantages and disadvantages especially in regard to detection of surface versus interior cracks.

Comparisons (1) between calculated and measured values of R (or ΔT_c) for monolithic Al_2O_3 give a calculated value of $84^\circ C$ and measured value of $200^\circ C$. Similar differences were noted for monolithic SiC with the calculated values always less than the measured values. Differences between the ideal and actual quenching conditions is the cause of this discrepancy and a correction term is added to the calculated values to compensate for this difference. This correction is $f(\beta)$ where $\beta = r_o h/k$, r_o is the relevant semidimension of the sample, h the heat transfer coefficient of the environment and k is the thermal conductivity of the material. The function $f(\beta) = 1.5 + 4.67/(\beta - 0.5 \exp(-51/\beta))$. For rapid quenching conditions β is large and $f(\beta)$ is approximately 1.5. A similar value can be assumed for the rapid heating resulting from a plasma discharge. Wang and Singh [1] reported ratios between the calculated and experimental values of R for Al_2O_3 and SiC as 2.4 and between 1.9 and 3.8, respectively. Clearly, a $f(\beta)$ of 1.5 is too small to correct the difference between the calculated and measured values.

Thermal Shock of Monolithic Ceramics

There have been extensive studies of the thermal shock behavior of monolithic ceramics because this is a critical property for many applications. Wang and Singh [1] have reviewed this literature for SiC and Al_2O_3 and their conclusion is that their thermal shock behavior has been found to be in good agreement with theory especially with the Hasselman unified theory [2]. Wang and Singh [1] compared the thermal shock behavior of SiC produced by CVD, hot pressing and pressureless sintering. Monolithic SiC produced by chemical vapor deposition (CVD) comes closest to being representative of the matrix of a SiC/SiC composite made by chemical vapor infiltration. The thermal shock was measured by residual flexure strength following quenching. The CVD SiC exhibited a strength increase following the thermal quench, the hot-pressed material exhibited a distinct T_c of about $500^\circ C$, and the sintered material showed a gradual strength decrease. The lack of a strength decrease for the CVD SiC quenched from temperatures up to $1000^\circ C$ was suggested as being a result of surface flaw healing during the heating step and the sample being too small to give the needed thermal stresses for a ΔT_c higher than $1000^\circ C$. The CVD SiC had a room temperature thermal conductivity of 250 W/m-K while the hot-pressed material had a room-temperature thermal conductivity of 87 W/m-K . The thermal conductivity affects the value of β , as described above, but for severe quench conditions where $\beta \gg 1$, the $f(\beta)$ approaches 1.5 independent of the thermal conductivity. For $\beta < 1$ the value R' is a function of thermal conductivity as given by equation three below:

$$R' = \sigma_t (1-\nu)k / \alpha E \quad (3)$$

where k is the thermal conductivity.

Takeda and Maeda [3] evaluated the effect of thermal conductivity on the thermal shock behavior of SiC by adding BeO and AlN to hot-pressed SiC material. The thermal conductivities with these additives were 100 W/m-K and 65 W/m-K , respectively while the ΔT_c 's were 680 and $450^\circ C$, respectively. This is in comparison to a ΔT_c of about $500^\circ C$ for hot-pressed material tested by Wang and Singh [1] with a thermal conductivity of 87 W/m-K . These results are qualitatively consistent with Equation 3 with increasing thermal conductivity resulting in an increasing R' . Since the materials were not made from the same starting powder or with the same hot-pressing conditions a quantitative correlation is not possible but a linear relationship between R' and κ is suggested.

Thermal Shock of Ceramic Composites

Thermal shock studies have been conducted on particle, whisker, and fiber reinforced ceramic matrix composites. Lee and Case [4] studied the thermal shock behavior of SiC whisker reinforced Al_2O_3 and showed that there was a gradual increase in the internal friction and decrease in the elastic modulus with increasing number of thermal cycles. These changes are

presumably the result of thermal shock induced microcracks. Tiegs and Becher [5] found that the addition of 20 % SiC whiskers to Al_2O_3 produced a material that exhibited no loss in strength following a single ΔT of 900°C while there was minor strength loss after 10 cycles at a ΔT of 300°C . The composite material had a fracture strength of 620 MPa while the monolithic material had a flexure strength of 310 MPa.

Wang and Singh [1] concluded that fiber reinforced ceramic composites possess superior thermal shock resistance in comparison with monolithic ceramics. Catastrophic failure is averted with these materials. These conclusions are supported by several studies of composites with continuous fiber reinforcement of SiC, glass and Si_3N_4 . Only the SiC/SiC composite results will be summarized since the thermal shock behavior of composites is dependent on the difference in thermal expansion between the fiber and matrix in addition to the thermal stress from the thermal gradient.

Wang and Singh [6,7] measured the retained flexural strength of SiC/SiC composites quenched from temperatures up to 1000°C , Figure 1. The composites were reinforced with Nicalon (presumably CG given the date of the reference) and CVI and polymer derived matrices with the fibers woven in a two-dimensional fabric. The composite with the CVI matrix had a ΔT_c of about 750°C while the composite with a polymer derived matrix had a ΔT_c of 400°C . These ΔT_c were defined by a decrease in the residual strength but the decrease was gradual and not discontinuous, as observed for monolithic material. Even with a ΔT of 1000°C the residual strengths were 85% and 75%, respectively for the CVI and polymer derived matrix material. These results suggest that the polymer derived SiC matrix has a lower matrix fracture strength than does the CVI matrix material. However, this is not the case since the matrix cracking stress is 150 MPa for the CVI material and 250 MPa for the polymer derived matrix material. Wang and Singh [7] explain the difference in the thermal shock response of these two composites as resulting from different damage processes. They suggest that debonding between the fiber and matrix controls the thermal shock behavior of the CVI material while fiber damage is suggested for the polymer derived matrix composite.

Lamicq et al. [8] also evaluated the thermal shock behavior of two-dimensional SiC/SiC composites with a CVI SiC matrix. These materials exhibited a residual strength of 85% following a quench with a ΔT of 300°C with no further decrease up to 1200°C . Fitzer and Gadov [9] also showed that a composite with unidirectional SiC fibers produced by CVD and a matrix produced by CVI resulted in a thermal shock resistance parameter $2\frac{1}{2}$ times greater than that of hot-pressed SiC.

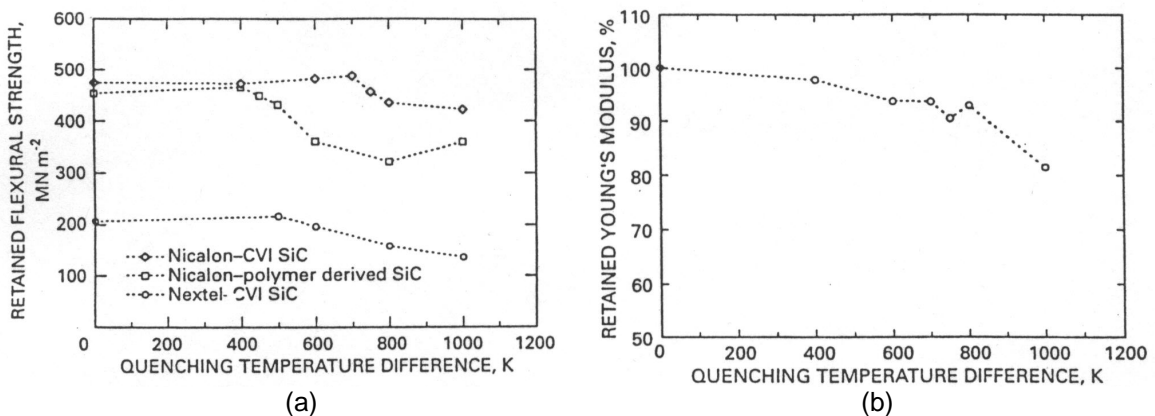


Figure 1. (a) Retained flexural strength v. quenching temperature difference for various continuous fibre reinforced ceramic composites, (b) Effect of quenching temperature difference on retained Young's modulus of NicalonTM fibre-CVI SiC composite.

Quenching from an elevated temperature into water or ice water is the standard method for evaluating the thermal shock of ceramics and ceramic composites; however, this is not prototypical for the heating cycle resulting from a plasma discharge that will result in a $+\Delta T$ rather than a $-\Delta T$. Eckel et al. [10] evaluated the thermal shock behavior of SiC/SiC as a result of a $+\Delta T$. They used a H_2-O_2 burner rig with ΔT ranging from 1300 to 2300°C. The thermal shock was created by rapid heating in contrast to other reported thermal shock tests where thermal shock was created by rapid cooling. Monolithic SiC failed in 1.5 cycles at a heating rate of 1400°C/s while SiC/SiC composite withstood 25 cycles with a 1700°C/s heating rate with little or no decrease in the tensile strength. A 35% strength loss was noted after 25 cycles with a 1900°C/s heating rate, but this effect was related to erosion and not composite cracking, Figure 2.

In summary, continuous fiber reinforced SiC/SiC composites exhibit excellent thermal shock resistance in both the standard thermal shock test with a $-\Delta T$ and in a non-standard test conducted by Eckel et al. (8) with a $+\Delta T$. The composite material does not exhibit a drastic drop in strength as do monolithic ceramics while they do retain 75% or more of their original strength following ΔT 's of up to 1200°C.

Models for Thermal Shock Behavior of Ceramic Composites

Thermal stresses in ceramic composites are the result of both the thermal gradient, as with monolithic ceramics, plus the mismatch in thermal expansion between the matrix and fiber. Boccaccini [11] has given the following relationship for a ceramic composite that considers the matrix stress resulting from the thermal gradient and thermal expansion mismatch inducing matrix cracking. There may be some conditions where fiber failure may occur prior to matrix failure although the fibers are stronger than the matrix in most ceramic composites. Also, fiber/matrix interface failure would decrease the strength of the composite but the relationship by Boccaccini [11], Equation 4, does not address this failure possibility.

$$\Delta T_c = (1-\nu) \{ (K_{Ic,m}/2[(r+s)/\pi]^{1/2}) - E_m \Delta \alpha \Delta T_F / [1 + E_m(1-V_f)/E_f V_f] \} / C E_e \alpha_e \quad (4)$$

Where the subscripts m, f and e refer to the matrix, fiber and effective values, V is volume fraction, and C is a non-dimensional constant that is a function of the Biot modulus β , r is the fiber radius, s is the average fiber spacing and ΔT_F is the temperature difference between room and the fabrication temperature. The variable $K_{Ic,m}$ is the matrix fracture toughness.

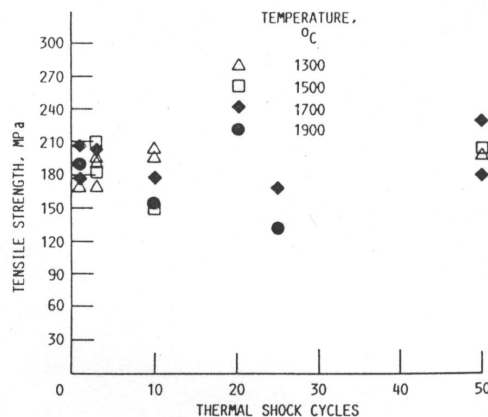


Figure 2. Retained room temperature tensile strength of Nicalon®/SiC ceramic composites after thermal shock.

Assuming the values listed in Table 1, Equation 4 predicts a ΔT_c of 957K. This value is 200K greater than the 750K reported by Wang and Singh [6,7]. There are several possible factors for this difference: 1) temperature dependence of α , 2) uncertainty in the $K_{Ic,m}$ and 3) the $f(\beta)$ correction as described above. Senor [12] has reported a value for α of $3.0 \times 10^{-6} K^{-1}$ for Morton CVD SiC at 25°C and $4.65 \times 10^{-6} K^{-1}$ at 1100°C. Factoring in the temperature dependence of α decreases the ΔT_c from 957K to 766K a value much closer to that reported by Wang and Singh [6,7]. A fracture toughness value of $5 \text{ MPa m}^{1/2}$ was used for this calculation but Morton lists a value of $3.3 \text{ MPa m}^{1/2}$ for CVD-SiC as measured by micro indentation while Carborundum lists a value of $4.6 \text{ MPa m}^{1/2}$ for Hexaloy SiC using a single edge notch bend specimen. Using the lower value, Equation 4 predicts a ΔT_c of 504K. With a fracture toughness of $5.0 \text{ MPa m}^{1/2}$, temperature dependence of α and $f(\beta)$ considered the calculated ΔT_c is 1077K while with a fracture toughness of $3.3 \text{ MPa m}^{1/2}$, temperature dependence of α and $f(\beta)$ factors considered, the calculated ΔT_c is 567K. These values bound the experimental values reported by Wang and Singh [6,7] and show that lower values of $K_{Ic,m}$ and larger values of α result in significant decreases in ΔT_c .

Radiation Effects on Thermal Shock of SiC/SiC Composites

There is no experimental data to assess the effects of radiation on thermal shock of SiC/SiC but there is data on the effects of radiation on their physical and mechanical properties. Radiation has been shown to reduce E and σ_r (13) but to have no effect on α (14). Recent radiation results for SiC/SiC composites, reinforced with radiation resistant Nicalon Type S fibers, have shown little loss in strength up to 10 dpa but prior work (13), with composites reinforced with Nicalon CG, showed a strength decrease of 50%. This loss in strength was due to two factors: 1) fiber shrinkage induced debonding from the matrix and 2) matrix microcracking during radiation. The value of E was also noted to decrease with radiation (13) but this decrease was due primarily to matrix microcracking and it is unclear how this will impact the value of ΔT_c . One approach to evaluating the effect of the microcracked matrix on thermal shock is to utilize the relationship for crack propagation in the matrix response to thermal shock as described by R'' in Equation 2. This equation shows that ΔT_c is inversely proportional to σ_r^2 unlike R' which is directly proportion to σ_r . Use of Equation 2 for $\sigma_{TS,c}$ in the relationship $\sigma_m = \sigma_{TS,c} + \sigma_r$ where σ_m is the stress induced in the matrix, $\sigma_{TS,c}$ is the composite thermal stress and σ_r is the residual stress in the matrix after fabrication. Using the approach by Boccaccini [11] to solve for ΔT_c does not result in a valid solution.

Assuming that radiation does not affect α , reduces σ_r by 50% that translates into a similar decrease in $K_{Ic,m}$, that the effect of radiation on E is through matrix microcracking and fiber

Table 1. Values Assumed for ΔT_c Calculation

Parameter	Value
C	0.5
ν	0.3
E_e	300 GPa
α_e	$3 \times 10^{-6} K^{-1}$
r	$5 \times 10^{-6} \text{ m}$
s	$10 \times 10^{-6} \text{ m}$
$K_{Ic,m}$	$5 \text{ MPa } \sqrt{\text{m}}$

debonding and that thermal shock does not cause further matrix microcracking and fiber debonding, the ΔT_c , from Equation 4, of irradiated material will decrease from 957K for unirradiated material to about 300K. This is a three-fold decrease with only a two-fold decrease in the fracture strength. Radiation was shown to decrease the thermal conductivity of SiC by a factor of three (13) but for rapid heating conditions as expected for a plasma discharge where the $\beta \gg 1$ there will be little effect of thermal conductivity on thermal shock performance.

Thermal Fatigue Behavior of Ceramic Composites

Thermal fatigue results from stresses induced during thermal cycling. These may be internal stresses or whole body stresses caused by material constraint. Thermal fatigue of materials in a fusion energy system will result from the shut-down/start-up cycles and the temperature change during the cycles. The frequency of these cycles will be determined by the duty cycle of the system and may be low frequency. There have been relatively few studies of the fatigue behavior of CMCs, and most of these have been conducted at high frequencies. Several factors affect the performance of composite materials in cyclic stress applications, for example: (1) compressive stress can cause delamination and microbuckling (15), and (2) tension-tension tests conducted at stresses below the matrix-cracking stress cause little fatigue damage (16). A regime where fiber interface sliding occurs has also been identified by Rouby and Reynaud [17] as causing fatigue damage in tests on 1D SiC/SiC tested at a frequency of 1 Hz and room temperature. Rouby and Reynaud [17] observed an endurance limit at which failure did not occur after 250,000 cycles and a regime where fatigue damage and failure occurred after 5 to 12,000 cycles. The endurance limit observed by Rouby and Reynaud [17] exceeded the matrix-cracking stress by about 30% in contrast to the results of Holmes [16] who observed an endurance limit equal to the matrix-cracking stress.

Kostopoulos et al. [18] measured the high cycle fatigue behavior of a 3D SiC/SiC composite and developed a power-law equation describing the dependence of the number of cycles to failure, N_f , on the applied stress. The tests were conducted at room temperature in air so there should not be an environmental degradation issue. The tests were conducted at a frequency of 10 Hz and a ratio of minimum to maximum stress, R, of 0.1. A value of N_f of 10^6 cycles corresponds to an applied stress of 85% of the ultimate strength. So clearly, there is little fatigue damage in these materials at room temperature. The following power-law relationship was derived from these results:

$$\sigma_{\text{applied}} / \sigma_{\text{ult}} = a N_f^{-k} \quad (5)$$

where σ_{applied} is the maximum applied stress during the fatigue test, σ_{ult} is the ultimate tensile strength of the composite, a is a constant and k is the fatigue strength exponent. Values of a = 2.21 and k = 0.04481 were reported by Kostopoulos et al. [18].

The fatigue behavior at an intermediate loading frequency of 0.25 Hz and at elevated temperature was evaluated by Forio and Lamon [19]. These tests were conducted in air so there is some possibility that there is an environmental effect on Forio and Lamon's [19] results but the material has a B addition to promote the formation of a borosilicate glass to seal the microcracks and protect the fibers and fiber/matrix interface. The tests were conducted at 0.25 Hz, an R value of 0.1 and at 600 and 1100°C. Tests at 1100°C and a maximum stress of 150 MPa resulted in a lifetime of 4.6×10^4 cycles while a stress of 220 MPa in a lifetime of 1.7×10^3 cycles. The authors report the matrix cracking in the transverse tows occurs at a stress of 150 MPa and matrix cracking in the longitudinal tows at 220 MPa. This change in matrix cracking pattern is likely the cause of the substantial decrease in lifetime with the increase in stress. The elastic modulus decreased by only 12% during the course of the test at 1100°C and a stress of 150 MPa. The composite lifetimes were shorter for tests and the drop in the elastic modulus greater at 600°C relative to 1100°C. For instance, for a maximum stress of 150°C the lifetime at 600°C was only

1.3×10^4 . This decrease in lifetime at 600°C is likely the result of the greater viscosity of the borosilicate glass at the lower temperature and therefore, it is less effective in filling in the cracks and protecting the fibers and fiber/matrix interfaces.

Results of low cycle fatigue tests conducted on SiC/SiC at 1100°C in a high-purity Ar environment [20] are shown in Figure 3. This test was conducted at a R value of 0.1 and with 1000 s hold time at load $f = 10^{-3}$ Hz and 25 cycles at each stress intensity value. Crack velocity decreased with increasing number of load cycles at low stress intensity, as demonstrated by the crack velocities after the first and 25th load cycle. This effect was diminished at high stress intensities. The decrease in crack velocity at low stress intensities is understood from observations of decreasing crack velocity as a function of hold time at constant load. This effect results from creep relaxation of the bridging fibers and the resulting increase in the number of fibers bridging the crack. The convergence of the two curves in Figure 3 at high stress intensity results either from fatigue damage with increasing number of cycles or from the fracture of bridging fibers that occurs for either constant or cyclic loads with increasing stress intensities. The crack velocity for the cyclically-loaded specimen is less than that for a statically-loaded specimen over the entire Stage II region. Therefore, it would appear that there was no fatigue damage for this test. Rouby and Reynaud [17] noted that fatigue failure was commensurate with a decrease in the tangential Young's modulus during high-cycle fatigue in 2D SiC/SiC composites. In the results given in Figure 3, the elastic modulus decreased by 20% between the first and last cycle. However, some decrease in modulus is expected as the stress intensity approaches Stage III because of fracture of the bridging fibers. More testing, conducted under constant K conditions, is required to determine the conditions that induce low-cycle fatigue damage of SiC/SiC at elevated temperatures.

Holmes et. al. [21], measured the cyclic creep or low cycle fatigue behavior of SiC fiber reinforced Si_3N_4 at 1200°C for several cycles of creep and recovery times. They found that there were fewer fiber failures when there was a recovery cycle (i.e., the load reduced to $0.01 P_{\max}$) as compared to either static load or cycling without any hold time during the unloaded period. For instance, there were 10% fiber failures for samples loaded 300 s and unloaded 300 s, 30% fiber failures for samples loaded 50 h and unloaded 50 h and 40% fiber failures for sustained loads. They attributed the reduced number of fiber failures to the reduction of fiber stress that occurs during

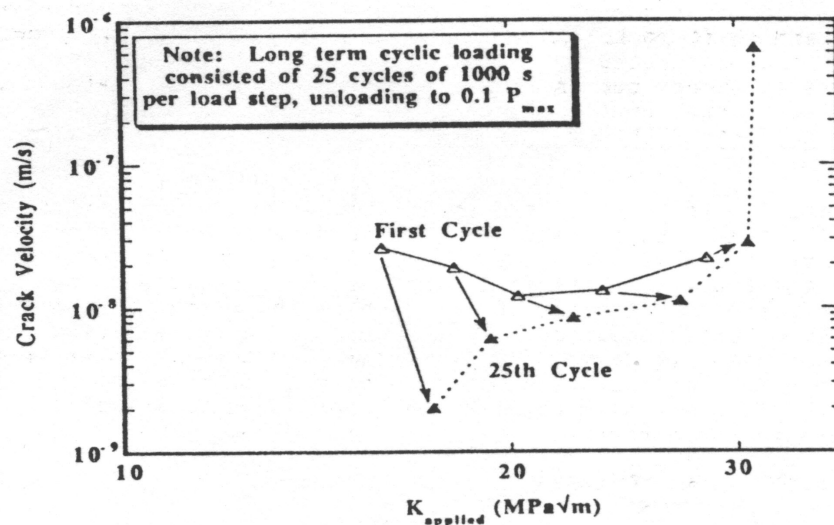


Figure 3. Low cycle fatigue behavior for a SiC/SiC Composite at 1100°C.

the recovery period. The results of Holmes et al. are similar to those of Jones and Henager [20] where the crack growth rates decreased with increasing number of cycles at a given stress intensity. The creep relaxation of the fibers with time and the greater amount of time associated with increasing number of cycles contributed to this decrease.

Wortherm [22] conducted a thermal fatigue test of enhanced SiC/SiC composite material with a temperature change between 600 and 1100°C. A load was also applied to simulate the constraint factor with a stress ratio (minimum to maximum stress) of zero. Both the load and temperature wave forms were triangular with a period of five minutes (frequency of 3×10^{-3} Hz). The stress was applied both in phase with the temperature cycle and 180 out of phase with the temperature cycle. All tests were conducted in laboratory air and in most high-temperature tests of SiC/SiC material, oxidation embrittlement or other environment induced degradation processes dominate the mechanical properties. These degradation processes are not representative of the conditions in a fusion energy system with a high-purity He coolant. However, the results of Wortherm were conducted on enhanced SiC/SiC that contained glass-forming elements that promotes glass formation to protect the fibers from damage by flowing into the matrix microcracks. Coated materials were also evaluated and these samples can also help isolate material behavior from environmental effects. The results of this study showed that the number of cycles to failure, N_f , decreased with increasing applied stress. Specifically for uncoated material and the stress applied out of phase, the N_f was 100 at a stress of 150 MPa and 1000 at a stress of 90 MPa. Coated samples had an N_f about three times higher than the uncoated samples suggesting that environmental effects were a factor in the properties of the uncoated samples. Fitting equation five to this data gives values of $a = 5.917$ and $k = 0.2840$. The larger value of k for the thermal fatigue results compared to high cycle fatigue results given by Kostopoulos et al. [18] illustrates the larger dependence of the applied stress on the cycles to failure. The room temperature, high cycle fatigue results reported by Kostopoulos et al. [18] exhibited a nearly flat curve of applied stress vs. cycles to failure above about 6×10^5 cycles.

The temperature cycle studied by Wortherm [21] is probably not the same as expected in a fusion energy system but the ΔT of 500°C may not be too different. Therefore, these results are fairly relevant for a fusion energy system. The proportional limit reported for this material was 60-80 MPa and many designs consider this the limiting stress for these materials. With a maximum stress of 80 MPa the thermal fatigue N_f is at least 3000 cycles based on the uncoated results and could be 10,000 cycles based on the coated results. Also, a few tests were conducted with a ΔT of 600°C with only a small decrease in the N_f . Therefore, the results of Wortherm [22] and Jones and Henager [20] suggest that thermal fatigue or low-cycle fatigue is not a serious issue for SiC/SiC composites for fusion applications.

REFERENCES

- [1] H. Wang and R. N. Singh, "Thermal Shock Behavior of Ceramics and Ceramic Composites," Intl. Materials Reviews, Vol 39, No. 6 (1994), p. 228-244.
- [2] D. P. .H. Hasselman, J. Am. Ceram. Soc., 52 (1969) p. 600-604.
- [3] Y. Takeda and K. Maeda, J. Ceram. Soc., Jpn, Intl. 99 (1991) p. 1113-1116.
- [4] W. J. Lee, E. D. Case, Mater. Sci. Eng., A119, (1989), 113.
- [5] T. N. Tiegs, and P. F. Becher: J. Am. Ceram. Soc., (1987), 70, C109-C111.
- [6] H. Y. Wang and R. N. Singh, Ceram. Eng. Sci. Proc., 15 (1994) p. 292-302.
- [7] H. Y. Wang and R. N. Singh, J. Am. Ceram. Soc., 79 (1996) p. 1783-92.

- [8] P. J. Lamicq, G. A. Bernhart, M. M. Dauchier and J. G. Mace, Am. Ceram. Soc., Bull., 65 (1986) p. 336-338.
- [9] E. Fitzner and R. Gadow, Am. Ceram. Soc., Bull., 65 (1986) p. 326-35.
- [10] A. E. Eckel, T. P. Herbell, E. R. Generazio, and J. Z. Gyenkeyesi, Ceram. Eng. Sci. Proc., (1991), 12, p. 1500-1508.
- [11] A. R. Boccaccini, Scripta Mater., Vol. 38 (1998) p. 1211-1217.
- [12] D. Senior, Pacific Northwest National Laboratory, private communication.
- [13] R. H. Jones, D. Steiner, H. L. Heinisch, G. A. Newsome and H. M. Kerch, J. of Nucl. Mater., 245 (1997) p. 87-107.
- [14] G. Youngblood, Pacific Northwest National Laboratory, private communication.
- [15] E. Bakis and W. W. Stinchcomb, in Composite Materials: Fatigue, Fracture, ASTM STP 907, ed. H. T. Hahn, American Society for Testing and Materials, Philadelphia, PA. 1986, p. 314.
- [16] J. W. Holmes, J. Am. Ceram. Soc., 74, (1991) p. 1639.
- [17] D. Rouby and P. Reynaud, in Proc. Conf. On High Temperature Ceramic Matrix Composites held at the 6th Eur. Confer. On Composite Materials, Bordeaux, Sept. 20-24, 1993, p. 499.
- [18] V. Kostopoulos, L. Vellios and Y. Z. Pappas, "Fatigue Behavior of 3-d SiC/SiC Composites," J. of Materials Science, 32 (1997) p. 215-220.
- [19] P. Forio and J. Lamon, "Fatigue Behavior at High Temperatures in Air of a 2D SiC/SiC-B-C Composite with Self-Healing Multi-layered Matrix," J. Am. Cer. Soc., in press.
- [20] R. H. Jones and C. H. Henager, Jr., Fusion Reactor Materials Semiannual Progress Report for period ending March 31, DOE/ER-0313/14, 1993, p. 451.
- [21] J. W. Holmes, Y. H. Park, J. W. Jones, J. Am. Ceram. Soc., 76 (1993) p. 1281.
- [22] D. W. Worthem, "Thermomechanical Fatigue Behavior of Coated and Uncoated Enhanced SiC/SiC," presented at 7th annual HITEMP Review, 1994, NASA Lewis Research Center, p. 66-1.